The Geometry of the Fixed-Point Set of the Einstein–Hilbert Flow with Matter: a Cuspidal Cubic, a Bogdanov–Takens Point and a Periodic Renormalization-Group Orbit

L. E. Pavesi* [1]

[1]Independent Researcher, Italy

October 11, 2026

Abstract

We study the dependence of the ultraviolet fixed point of the derived Einstein–Hilbert flow with minimally coupled matter (optimised cutoff, harmonic gauge) on the matter content (X, Y), treating X and Y as continuous parameters. Three exact results are proved. (i) The fixed-point set is a ruled surface; the saddle–node (fold) curve in the (X, Y) plane, which bounds the existence region found numerically in the author's book on Quantum Distortion Gravity, is a cuspidal cubic, i.e. the semicubical parabola in suitable affine coordinates, with a cusp at the rational point $(X, Y) = (12349/15552, -126613/23328)$ and an explicit rational parametrisation; for any regulator it is the Legendre transform of a function of λ. (ii) At a fixed point the determinant of the stability matrix equals $2F'(u)/(3u^2N\omega)$, where F is the fixed-point cubic, so the Poincaré index of every admissible fixed point is the sign of F'. (iii) The trace of the stability matrix has a closed form; its zeros on the fold curve are the roots of an explicit quartic, two of which are admissible Bogdanov–Takens points, one at $(X, Y) \simeq (4.017, -5.345)$ with $(g_*, \lambda_*) \simeq (1.869, 0.0169)$. From it emanates a Hopf curve with first Lyapunov coefficient positive (subcritical) at all 19 points sampled along it $(4.1 \leq X \leq 130)$, so that on the side where the fixed point is ultraviolet attractive it is surrounded by an unstable periodic orbit of the flow, bounded by a homoclinic loop of the saddle. The periodic orbit, the Hopf and homoclinic curves, and the transition to a repulsive focus are established numerically, not proved. The cusp and the Bogdanov–Takens point persist for six regulators tested; the contents assigned to Quantum Distortion Gravity (n_f Dirac fermions plus two Proca fields, or two massless vectors) never reach any of these structures. All statements concern the truncated flow and are not claims about the full theory.

Keywords: asymptotic safety, functional renormalization group, fixed point, matter content, cusp, Bogdanov–Takens bifurcation, limit cycle

1 Introduction

In the Einstein–Hilbert truncation of the functional renormalization group, the non-Gaussian fixed point (g_*, λ_*) depends on the matter content only through two numbers, X and Y (Section 2). Earlier work on Quantum Distortion Gravity (QDG) [9] located, numerically and partly in closed form, the region of the (X, Y) plane in which an admissible fixed point exists. This paper asks a different question: what is the *shape* of the object that the fixed point defines when (X, Y) varies, and what dynamical structure does the flow acquire around it? The answer turns

*Corresponding author e-mail: lucapv02@gmail.com

out to contain a small number of classical geometric figures: a ruled surface, a cuspidal cubic (Neile's semicubical parabola), a Bogdanov–Takens point, an algebraic Hopf curve, a homoclinic curve, and a closed orbit of the flow in the (g, λ) plane.

Logical status. Headings and statements carry the tags `[PROVED]` (proved here by hand), `[EXACT]` (obtained with exact rational arithmetic by a script and checked at many rational points), `[NUMERICAL]` (computed numerically, not proved), `[INPUT]` (taken from a source) and `[OPEN]`. The scripts are in the folder `code/`; `verify_all.py` re-checks every exact statement.

What is new and what is not. The existence region of the fixed point in the (X, Y) plane, its boundary by the pole arc of η in closed form, and the numerical saddle–node arc are in [9]. Phase portraits of the Einstein–Hilbert flow without matter are classical [1]. What I could not find in the sources I consulted [1, 3, 4] (and in a few web searches using the terms "catastrophe", "cusp", "fold" and "bifurcation" together with asymptotic safety) is the exact description of the fold curve, the index formula, the Bogdanov–Takens point and the periodic orbit below. This is not a literature survey; I make no priority claim.

Scope. Everything refers to the *derived* Einstein–Hilbert flow of the book [9] (Litim cutoff, $\alpha = 1$, linear split, background S^4, minimal matter in the "type B" counting), with X, Y real. The Weyl-gauged QDG sector is not in this flow and whether it modifies it is an open problem. The structures found here lie at contents (X, Y) that the QDG families n_f Dirac fermions + two Proca fields (or + two massless vectors) *do not reach* (Proposition 3.4); they are properties of the flow as a mathematical object, not of QDG.

2 The flow and the fixed-point cubic `[INPUT]`

Let $g = G_k k^2$, $\lambda = \bar{\Lambda}_k / k^2$, $t = \ln k$, $u = 1 - 2\lambda$. The derived flow is

$$\beta_g = \frac{\mathrm{d}g}{\mathrm{d}t} = (2 + \eta)\, g, \qquad \eta = \frac{g\,(B_1 + X/6\pi)}{1 - gB_2}, \tag{1}$$

$$\beta_\lambda = \frac{\mathrm{d}\lambda}{\mathrm{d}t} = -(2 - \eta)\lambda + \frac{g}{2\pi}\Big[\frac{5}{u} - 4 - \frac{5\eta}{6u}\Big] + \frac{Yg}{4\pi}, \tag{2}$$

with $B_1 = \frac{1}{3\pi}\big[\frac{5}{u} - \frac{9}{u^2} - 7\big]$, $B_2 = -\frac{1}{12\pi}\big[\frac{5}{u} - \frac{6}{u^2}\big]$ (Reuter [1], optimised cutoff [2]; see [9], Part IV). The matter enters through $X = N_S + 2N_D - 4N_V - 3N_P$ and $Y = N_S - 4N_D + 2N_V + 3N_P$ (real scalars, Dirac fermions, massless vectors, Proca fields). I put $\omega := 1 - gB_2$. A fixed point is *admissible* if $g > 0$, $u > 0$, $\omega > 0$.

Setting $\eta = -2$ gives $g = 2\pi/N(u)$ with $N(u) = \frac{4}{u^2} - \frac{5}{2u} + \frac{c}{6}$, $c := 14 - X$, and then $\beta_\lambda = 0$ is equivalent to $F(u) = 0$,

$$F(u) = 2c\,u^3 - (2c + 54 - 3Y)\,u^2 + 118\,u - 48. \tag{3}$$

Moreover $\omega N = M(u) := \frac{3}{u^2} - \frac{5}{3u} + \frac{c}{6}$, so that for $N > 0$ admissibility means $N > 0$ and $M > 0$ (this is the cubic and the three conditions of the book, Part IV; the identities used below are re-derived in the proof of Proposition 4.1). The critical exponents are $\theta_i = -\mathrm{eig}(J)$, $J_{ij} = \partial\beta_i/\partial x_j$ at the fixed point; θ with positive real part is ultraviolet (UV) attractive. In what follows $s := 1/u$.

3 The ruled surface and the cuspidal cubic

Proposition 3.1 (Ruled surface and fold curve `[PROVED]`)**.** *(a) Equation* (3) *is linear in* (X, Y)*. For fixed* u *it describes the straight line*

$$Y = 18 - \frac{118}{3u} + \frac{16}{u^2} + \frac{2}{3}(u-1)(X-14) \tag{4}$$

in the (X, Y) *plane. Hence the set of fixed points* $\Sigma = \{(X, Y, u) : F(u) = 0\}$ *is a ruled surface, a graph over the* (X, u) *plane.*

(b) The projection $\Sigma \to (X, Y)$ *is singular exactly where* $F'(u) = 0$*. The image of the singular set is the curve* Γ*,*

$$X(s) = 14 - 59s^2 + 48s^3, \qquad Y(s) = 18 - \frac{236}{3}s + \frac{262}{3}s^2 - 32s^3, \qquad s = \frac{1}{u} \in \mathbb{R}, \tag{5}$$

which is the envelope of the family (4)*. It is the zero set of the discriminant of* F*,*

$$D(X, Y) = 192(2X + 3Y)^3 + 25744X^2 + 212016XY - 299772Y^2 + 861088X - 3795504Y - 10946544 = 0. \tag{6}$$

F *has three real roots if* $D > 0$ *(inside the cusp) and one if* $D < 0$*.*

(c) Γ *has exactly one singular point, a cusp, at* $s = 59/72$*, i.e.* $u_c = 72/59$*,* $\lambda_c = -13/118$*,*

$$(X_c, Y_c) = \Big(\frac{12349}{15552}, -\frac{126613}{23328}\Big) \simeq (0.79405,\ -5.42751), \tag{7}$$

where F *has a triple root. In the affine coordinates* $\xi = \frac{(2X+3Y)-(2X_c+3Y_c)}{144}$*,* $\zeta = \frac{\frac{26}{3}(X-X_c)-59(Y-Y_c)}{2304}$ *the curve is the semicubical parabola* $\xi^3 = \zeta^2$ *(parametrised by* $\xi = t^2$*,* $\zeta = t^3$*,* $t = s - \frac{59}{72}$*).*

Proof. (a) is read off from (3): $F = c\,(2u^3 - 2u^2) + 3Yu^2 - 54u^2 + 118u - 48$ with $c = 14 - X$. (b) Singularity of the projection is $\partial_u F = 0$. Solving $F = 0$ and $F' = 0$, which are linear in (c, Y), gives first $2cu^2 = 118 - 96/u$, i.e. $c = 59s^2 - 48s^3$, then (5). The discriminant of a cubic is a polynomial in its coefficients, which are linear in (X, Y); its expansion is (6) (computed exactly by interpolation, `t12_implicit.py`; the cubic part is $192(2X + 3Y)^3$, a perfect cube). (c) $X'(s) = 2s(72s - 59)$, $Y'(s) = -96(s - \frac{59}{72})(s - 1)$, which vanish together only at $s = 59/72$ (at $s = 0$, $Y' \neq 0$). Writing $X = X_c + 59t^2 + 48t^3$, $Y = Y_c + \frac{26}{3}t^2 - 32t^3$ one finds $2X + 3Y - 2X_c - 3Y_c = 144t^2$ and $\frac{26}{3}(X - X_c) - 59(Y - Y_c) = 2304\,t^3$. The numerical values X_c, Y_c and $F''' \neq 0$ are exact rational arithmetic. `verify_all.py` checks (a)–(c) at many rational points. □

Remark 3.2 (Whitney cusp)**.** The map $(X, u) \mapsto (X, Y)$ from the surface Σ to the plane has folds along Γ and one cusp; these are the generic stable singularities of maps between planes [5]. The fixed-point equation near the cusp is locally the normal form $x^3 + ax + b = 0$ of the cusp catastrophe.

Theorem 3.3 (Any regulator `[PROVED] given the book's fixed-point locus`)**.** *For a general cutoff shape, the fixed-point locus of the code of the book (`rre.py`) is, for each* λ*, a straight line in the* (X, Y) *plane,*

$$Y = -\kappa\,\lambda\,X + c(\lambda), \qquad \kappa = \frac{2\,\Phi_1^1(0)}{3\,\Phi_2^1(0)}, \tag{8}$$

($\kappa = 4/3$ *for the optimised cutoff, where* $c(\lambda) = 18 - \frac{118}{3u} + \frac{16}{u^2} + \frac{56}{3}\lambda$*). The fold curve is the envelope of this family, i.e. the Legendre transform of* c*:* $X = c'(\lambda)/\kappa$*,* $Y = c(\lambda) - \lambda c'(\lambda)$*, and its cusps are the inflection points* $c''(\lambda) = 0$*. For the optimised cutoff* $c'' = 0$ *gives* $u = 288/236 = 72/59$*, as above.*

Proof. The envelope of $Y = m(\lambda)X + c(\lambda)$ with $m = -\kappa\lambda$ is given by $m'X + c' = 0$, i.e. $X = c'/\kappa$, and $Y = mX + c$. Then $X' = c''/\kappa$ and $Y' = mX'$ (because $m'X + c' = 0$), so both derivatives vanish together iff $c'' = 0$. The linearity (8) is the structure used by `rre.py`; I checked numerically that the roots it produces solve the flow ($\max|\beta| \sim 5 \times 10^{-15}$ for the exponential regulator, $\alpha = 1$). □

Proposition 3.4 (The QDG families avoid the cusp `[EXACT]`)**.** *Along* $(X, Y) = (2n_f - 6,\ 6 - 4n_f)$ *(two Proca fields) and* $(2n_f - 8,\ 4 - 4n_f)$ *(two massless vectors),* D *is a cubic polynomial in* n_f *with a single real root, at* $n_f \simeq -68.5$ *and* -71.4 *respectively, and leading coefficient* $-98304 < 0$*. Hence* $D < 0$ *for all* $n_f \geq 0$*: the cubic* (3) *has exactly one real root, and neither family meets* Γ*.*

Proof. Substitute in (6): $D = -98304n_f^3 - 6168320n_f^2 + 38142080n_f - 56342208$ (resp. $-98304n_f^3 - 6536960n_f^2 + 34080000n_f - 42962800$); the remaining two roots are complex ($n_f \simeq 2.89 \pm 0.02i$, resp. $2.47 \pm 0.14i$). Script `t22_tables.py`. □

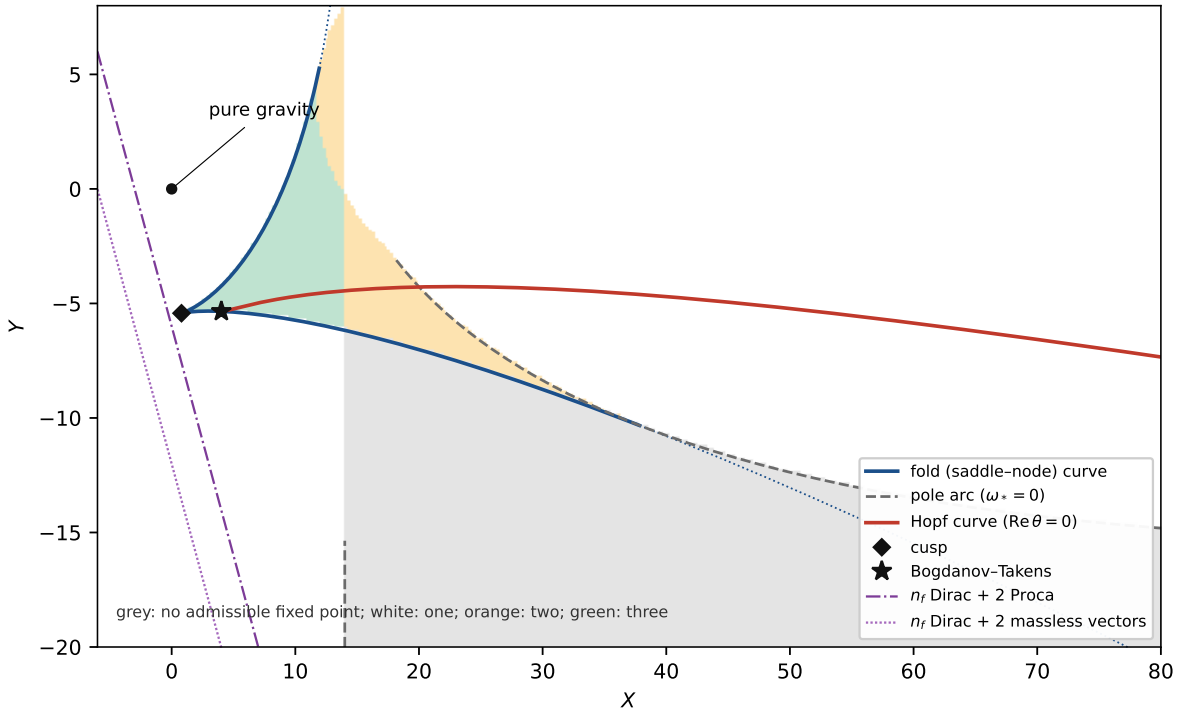


Figure 1: The (X, Y) plane. Shading: number of admissible fixed points. Blue: the fold curve Γ (full line where the fixed point on it is admissible), with the cusp (diamond) and the Bogdanov–Takens point (star). Red: Hopf curve $\Re\theta = 0$. Dashed grey: the pole arc and the line $X = 14$ of [9]. Purple: the two QDG families. Scripts `make_curves.py`, `make_figs.py`.

The two branches of Γ on either side of the cusp bound the wedge with three real roots. To the left of $X = 14$ the wedge contains three admissible fixed points (Figure 1); at $X = 14$ one root escapes to $u \to \infty$. The saddle–node arc of [9], which there was found by bisection, is the part $59/48 \leq s \leq (77 + \sqrt{4009})/96$ of the same curve Γ: indeed $X(59/48) = 14$, $Y(59/48) = 18 - 118^2/576 = Y_0 = -6.1736$ (the point at which that paper starts the arc, Proposition on $X = 14$), and $X\big((77 + \sqrt{4009})/96\big) = 37.84 = X_j$ is where the arc meets the pole arc.

4 The index of a fixed point [PROVED]

Proposition 4.1 (Determinant of the stability matrix)**.** *At an admissible fixed point,*

$$\det J = \frac{2\,F'(u_*)}{3\,u_*^2\,N(u_*)\,\omega_*}, \qquad \omega_* = \frac{M(u_*)}{N(u_*)}. \tag{9}$$

Hence $\operatorname{sign}\det J = \operatorname{sign} F'(u_*)$*, and the Poincaré index of the fixed point is* $+1$ *(node or focus) if* $F' > 0$ *and* -1 *(saddle) if* $F' < 0$*. In particular a zero exponent* $\theta = 0$ *occurs exactly on* Γ*.*

Proof. At a fixed point $2 + \eta = 0$, so $\det J = g\,(\eta_g\,\partial_\lambda\beta_\lambda - \eta_\lambda\,\partial_g\beta_\lambda)$. The nullcline $\eta = -2$ is the graph $g = G(\lambda) = 2\pi/N(u)$; differentiating $\eta(G(\lambda),\lambda) = -2$ gives $\eta_g G' + \eta_\lambda = 0$, hence $\det J = g\,\eta_g\,h'(\lambda_*)$ with $h(\lambda) = \beta_\lambda(G(\lambda),\lambda)$. From $\eta = gP/\omega$, $P = B_1 + X/6\pi$, one has $\eta_g = P/\omega^2$, and $\eta = -2$ means $gP = -2\omega$, so $\eta_g = -2/(g\omega)$ and $\det J = -2h'(\lambda_*)/\omega_*$. On the nullcline,

$$h = -4\lambda + \frac{1}{N}\Big(\frac{20}{3u} - 4 + \frac{Y}{2}\Big) = \frac{(2u-2)N + \frac{20}{3u} - 4 + \frac{Y}{2}}{N} = \frac{F(u)}{6u^2N(u)},$$

(the last step is a direct expansion: $6u^2\times$ numerator $= F$). At a zero of F, $h'(\lambda) = -2F'(u)/(6u^2N) = -F'(u)/(3u^2N)$, which gives (9). The identity $\omega N = M$ follows from $N - 2\pi B_2 = M$. I also verified (9) in exact rational arithmetic at 60 random (u,c) (`verify_all.py`). □

Corollary 4.2. *For* $c > 0$ *(that is* $X < 14$*) and three admissible fixed points* $u_1 < u_2 < u_3$*, the indices are* $(+1,-1,+1)$*: the middle one (in* u*) is a saddle and the outer ones are nodes or foci; the indices sum to* $+1$*. For* $c < 0$ *the pattern is reversed.*

Proof. The cubic F with leading coefficient $2c$ has F' of alternating sign at consecutive simple roots; for $c > 0$, $F'(u_1) > 0$. □

5 The trace, the Bogdanov–Takens points and the Hopf curve

Proposition 5.1 (Trace of the stability matrix [EXACT])**.** *At an admissible fixed point, with* $N = 4s^2 - \frac{5}{2}s + \frac{c}{6}$*,* $M = 3s^2 - \frac{5}{3}s + \frac{c}{6}$*,*

$$\operatorname{tr} J = \frac{T(s,c)}{N\,M}, \qquad T = -\frac{c^2}{6} + c\,\frac{65s - 29s^2 - 48s^3}{18} - \frac{50}{3}s^2 - \frac{115}{18}s^3 + \frac{332}{3}s^4 - 64s^5. \tag{10}$$

Derivation. Put $\tilde g = g/\pi$ (the flow depends on g,π only through g/π, and $\operatorname{tr},\det$ are invariant under this rescaling). At $\eta = -2$: $\tilde g = 2/N$, $P = -M$, $\eta_g = -N^2/M$, $\eta_\lambda = 2s^2(5-16s)/M$, whence $J_{gg} = -2N/M$, $J_{\lambda\lambda} = -4 + \eta_\lambda\big(\lambda - \frac{5s}{6N}\big) + \frac{40s^2}{3N}$ with $\lambda = \frac{s-1}{2s}$. Therefore $NM\operatorname{tr} J = -2N^2 - 4NM + s(5-16s)(s-1)N - \frac{5}{6}s^3(10-32s) + \frac{40}{3}s^2M$, which is quadratic in c; its expansion (done with exact rational functions, `ratfun.py`, `t19_hopf_closed.py`) is (10). The formula agrees with a finite-difference Jacobian to 2.5×10^{-15} at 100 random points. □

On Γ ($c = 59s^2 - 48s^3$) the numerator factorises as $T|_\Gamma = -\frac{s^2}{9}\,q(s)$,

$$q(s) = 2304s^4 - 7200s^3 + 6641s^2 - 1860s + 150. \tag{11}$$

Its real roots are $s = 0.142289,\ 0.262293,\ 1.035029,\ 1.685390$. The points of Γ at these s have $\det J = 0$ and $\operatorname{tr} J = 0$, so J is nilpotent. Two of them are admissible (Table 1); $J \neq 0$ there, so they are candidate Bogdanov–Takens (BT) points [6, 7].

BT_2 has $g_* \simeq 41$ and $N = 0.15$: it lies far outside any region in which the truncation can be trusted and I do not discuss it further. For BT_1 the normal-form coefficients, computed by finite differences with Kuznetsov's formulas [8] ($Aq_0 = 0$, $Aq_1 = q_0$, $\langle p_i, q_j\rangle = \delta_{ij}$), are

Table 1: Special points of the fold curve Γ (optimised cutoff). The exponents on Γ are $(\theta_1, \theta_2) = (0, -\operatorname{tr} J)$ except at BT.

	$s = 1/u$	λ_*	g_*	X	Y	θ_2
cusp	59/72	$-13/118$	2.2137	0.79405	-5.42751	1.497
BT_1	1.035029	0.016922	1.8692	4.01710	-5.34534	0
BT_2	0.262293	-1.40627	41.44	10.8071	2.7972	0

$a = \frac{1}{2}\langle p_1, B(q_0, q_0)\rangle = -2.092$ and $b = \langle p_0, B(q_0, q_0)\rangle + \langle p_1, B(q_0, q_1)\rangle = -0.414$, both non-zero and stable under change of step ($h = 10^{-3}, 4\times10^{-4}, 2\times10^{-4}$) `[NUMERICAL]`. The non-degeneracy condition on the parameters (regularity of the map $(X, Y) \mapsto (\beta_1, \beta_2)$) is not checked analytically; instead I verified numerically that the unfolding predicted for such a point is realised (Section 6).

Proposition 5.2 (Hopf locus `[EXACT]`). *Fixed points with* $\operatorname{tr} J = 0$ *and* $\det J > 0$ *(purely imaginary exponents* $\theta = \pm i\sqrt{\det J}$*) lie on the algebraic curve* $T(s, c) = 0$*, i.e.* $c = 3T_1 \pm \sqrt{9T_1^2 + 6T_0}$ *with* $T_1 = \frac{65s - 29s^2 - 48s^3}{18}$*,* $T_0 = -\frac{50}{3}s^2 - \frac{115}{18}s^3 + \frac{332}{3}s^4 - 64s^5$ *(the parts of* T *linear and independent of* c*); explicitly*

$$c_H(s) = \frac{65s - 29s^2 - 48s^3 \;\pm\; s\sqrt{Q(s)}}{6}, \qquad Q(s) = 2304s^4 - 11040s^3 + 18505s^2 - 5150s + 625, \tag{12}$$

and $(X, Y) = \big(14 - c_H,\ 18 - \frac{118}{3}s + 16s^2 - \frac{2}{3}\,c_H\,(\frac{1}{s} - 1)\big)$*. Q has no real root, so c_H is smooth for all real s. The branch with the $+$ sign passes through BT_1 and carries the physical Hopf points.*

Proof. $T = 0$ is a quadratic in c with discriminant $9T_1^2 + 6T_0 = s^2 Q(s)/36$ (exact). The $+$ branch reproduces the numerical Hopf points (checked for five points, `t19`). The last formula is Eq. (4) written with $u = 1/s$. □

6 The unfolding: Hopf, homoclinic loop and a periodic orbit `[NUMERICAL]`

Hopf curve. Starting at BT_1, the curve of Proposition 5.2 runs to $X = 4.1 \ldots 130$ (the range scanned), with $Y \in [-11.4, -4.27]$ and $0.85 \lesssim g_* \lesssim 1.8$. For the admissible fixed points on it, $\lambda_* \in (0.017, 0.33)$ and $\omega = \sqrt{\det J}$ increases from 0 at BT_1 to 24 at $X = 130$. The first Lyapunov coefficient ℓ_1 (Kuznetsov's formula, derivatives by finite differences, formula validated on normal forms with known ℓ_1 and on the Brusselator) is positive at all 19 points computed (Table 2); only its sign is used.

Consequence: a periodic orbit. Since $\ell_1 > 0$, each Hopf point is *subcritical*: on the side where the focus is UV attractive ($\operatorname{tr} J < 0$, $\Re\theta > 0$, i.e. larger Y near BT_1) there is an *unstable* periodic orbit surrounding it; on the other side there is none and the focus is UV repulsive. I confirmed this by integrating the flow (DOP853, rtol $= 10^{-11}$) in the direction of decreasing k, in which the orbit is attracting (script `cyc.py`, `t17_cycle_far.py`): at $X = 10, 22, 44$ and $Y = Y_H \pm 0.003, \pm 0.01$ the orbit is found for $\Re\theta > 0$, with period within 1% of $2\pi/\omega$ and an amplitude that grows with $\Re\theta$ (from 0.03–0.04 at $Y - Y_H = 0.003$ to 0.08–0.23 at 0.01), and absent for $\Re\theta < 0$. Near BT_1 (at $X = 4.2171$, $Y_H = -5.334775$) the amplitude in g and the period are:

$Y - Y_H$	5×10^{-4}	10^{-3}	2×10^{-3}	4×10^{-3}	8×10^{-3}	$8.86\times10^{-3} = Y_{\mathrm{hom}} - Y_H$
amplitude	0.0179	0.0253	0.0357	0.0501	0.0687	loop
period in $t = \ln k$	8.43	8.53	8.75	9.31	12.04	∞

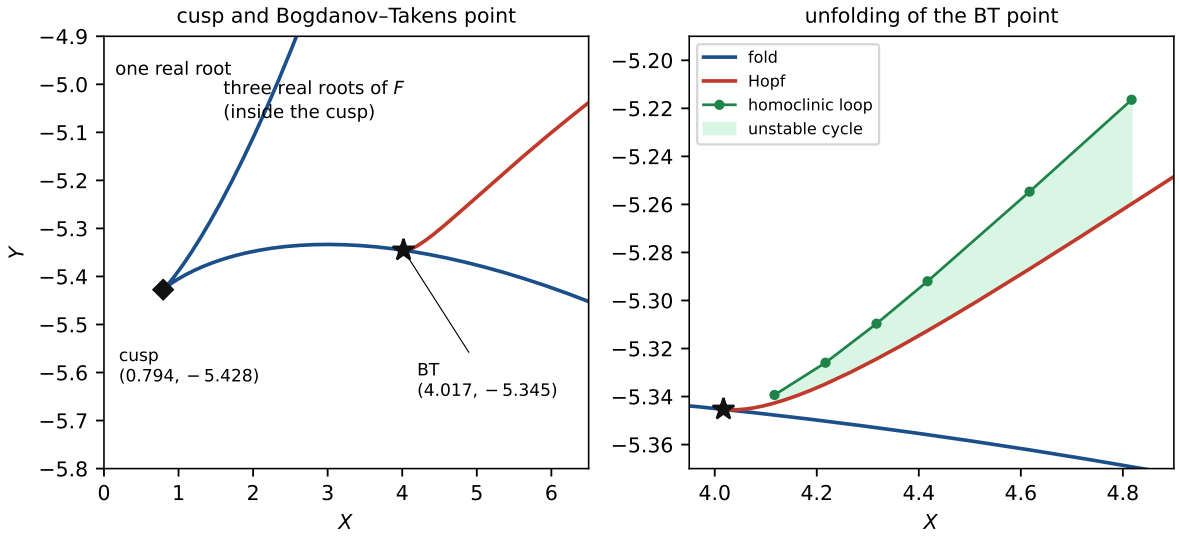


Figure 2: Left: the cusp and BT_1 on the cuspidal cubic (blue) with the Hopf curve (red) leaving BT_1 (apparently tangent to the fold). Right: the unfolding of BT_1. Green: homoclinic loop of the saddle (numerical points, Section 6); the shaded sliver, between the Hopf curve and the homoclinic curve, is where the UV attractive focus is surrounded by a periodic orbit.

Table 2: Points of the Hopf curve and the first Lyapunov coefficient ℓ_1 (its sign decides sub-/supercriticality; $\ell_1 > 0$: subcritical). Script `t16_l1_global.py`.

X	Y_H	g_*	λ_*	ω	ℓ_1
4.1	−5.3437	1.809	0.027	0.516	+1.720
5.0	−5.2347	1.540	0.074	1.395	+0.122
8.0	−4.8709	1.267	0.131	2.317	+0.048
10.0	−4.6910	1.183	0.151	2.698	+0.048
14.0	−4.4459	1.081	0.179	3.301	+0.063
22.0	−4.2666	0.978	0.213	4.268	+0.111
36.0	−4.5368	0.900	0.247	5.749	+0.219
52.0	−5.3412	0.864	0.271	7.454	+0.373
74.0	−6.8733	0.847	0.294	10.160	+0.674
100.0	−8.9506	0.844	0.312	14.544	+1.350
130.0	−11.4266	0.849	0.329	24.060	+4.033

At small $Y - Y_H$ the amplitude grows as $\sqrt{Y - Y_H}$ (ratio 1.416 between the first two columns, $\sqrt{2} = 1.414$) as in a Hopf bifurcation ($2\pi/\omega_H = 8.34$).

Homoclinic loop. The orbit grows until it touches the saddle S (the third fixed point of the wedge) and disappears. The existence of the orbit ends at $Y_{\mathrm{hom}} = -5.325912$ ($X = 4.2171$); independently, the unstable manifold $W^u(S)$ of the saddle changes from not ending in the focus to ending in it at $Y = -5.32591122$ (bisection, `t18_homoclinic.py`); the two values agree to 10^{-6}, so the end of the orbit is a saddle connection (homoclinic loop). The homoclinic points computed for six values of X are on the green curve of Figure 2; the sliver where the orbit exists has width $\simeq 10^{-2}$ in Y. This is the unfolding predicted for a non-degenerate BT point [8]: fold, Hopf curve tangent to it, homoclinic curve tangent to it.

Remark 6.1 (What the orbit is)**.** Figure 3(b): the periodic orbit is a closed trajectory of the

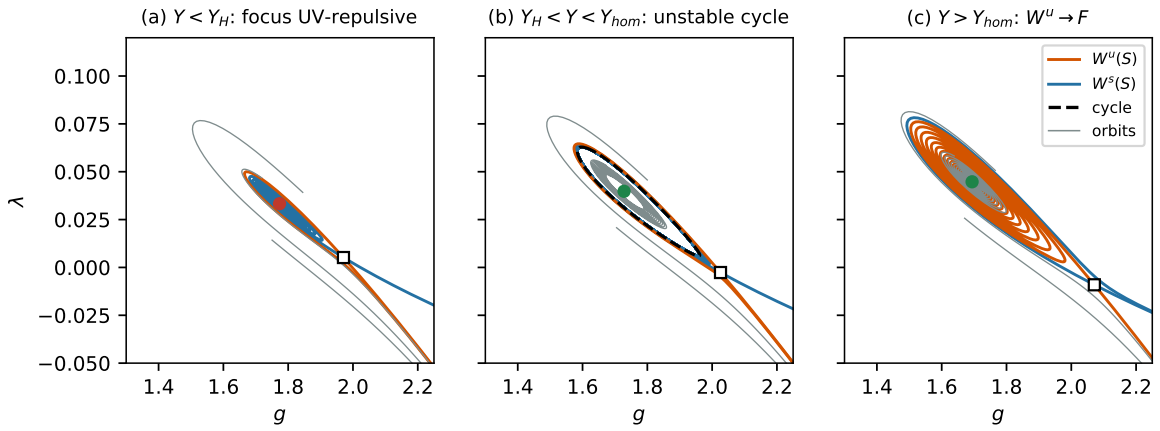


Figure 3: Phase portraits in the (g, λ) plane at $X = 4.2171$ ($t = \ln k$ increases towards the UV). (a) $Y < Y_H$: the focus is UV repulsive (the stable manifold W^s of the saddle winds into it in the backward direction). (b) $Y_H < Y < Y_{\rm hom}$: an unstable periodic orbit (dashed) surrounds the UV attractive focus and bounds its basin of attraction. (c) $Y > Y_{\rm hom}$: $W^u(S)$ is captured by the focus; the basin of the focus is bounded by $W^s(S)$. Script `make_fig3.py`.

truncated flow. Along it the couplings oscillate while k varies by a factor $e^{8.4}$ per period near BT_1 (and $e^{1.5}$ per period at $X = 22$). It is unstable towards the UV, so it is not itself a UV completion; its role is to bound the set of initial conditions flowing to the fixed point. Whether any analogue exists in the full theory is open.

7 Robustness with respect to the regulator [NUMERICAL]

By Theorem 3.3 the cusp is $c''(\lambda) = 0$ and the fold curve is a Legendre transform for any regulator. Using the regulator-general flow of the book (`rre.py`, copied unchanged as `rre_book.py`) I located the cusp and the points of the fold curve with $\mathrm{tr}\, J = 0$, for Litim cutoffs $R = a(k^2 - p^2)\theta(k^2 - p^2)$ and exponential cutoffs $R = \alpha\, p^2/(e^{p^2/k^2} - 1)$ (script `t20_regulators.py`). Table 3 gives the results. For $a = 1$ the numerical cusp and BT_1 agree with the exact values to the digits shown.

Table 3: Cusp and Bogdanov–Takens point BT_1 for six regulators (admissible in all cases, $\det J < 10^{-5}$ in absolute value at BT). For the Litim cutoffs the far point BT_2 ($g_* = 30$–56) also exists.

regulator	cusp (X, Y)	g_*	BT_1 (X, Y)	g_*	λ_*
Litim $a = 1$	$(0.794, -5.428)$	2.214	$(4.017, -5.345)$	1.869	0.0169
Litim $a = 0.7$	$(0.900, -5.633)$	2.458	$(4.238, -5.535)$	2.061	0.0111
Litim $a = 1.5$	$(0.658, -5.188)$	2.000	$(3.646, -5.123)$	1.703	0.0229
exponential $\alpha = 1$	$(1.232, -6.269)$	1.009	$(3.569, -6.168)$	0.850	−0.0330
exponential $\alpha = 1.5$	$(1.096, -6.127)$	0.844	$(3.756, -6.018)$	0.709	−0.0187
exponential $\alpha = 2$	$(1.003, -6.020)$	0.750	$(3.824, -5.910)$	0.629	−0.0068

So the cusp and a nilpotent point of the fold curve exist for all six, and for the exponential cutoffs at smaller couplings ($g_* \simeq 0.6$–0.85). Since a non-degenerate BT point is structurally stable in two-parameter families, small smooth deformations of the beta functions move it but do not remove it. What I did *not* do for the other regulators is the unfolding: the sign of ℓ_1, the position of the Hopf curve relative to BT_1 and the existence of the orbit were examined only for

the optimised cutoff. For the exponential cutoff $\alpha = 1$ the trace of the focus does change sign close to the fold on the side $X < X_{\rm BT}$ (`t23_reg_trace_map.py`), i.e. the Hopf curve appears to leave BT_1 towards smaller X, opposite to the Litim case; this has not been followed further.

8 Which matter contents reach these structures [NUMERICAL]

Since X, Y come from integer (half-integer for N_D) counts, I scanned $N_S \le 40$, $N_D \in \{0, \frac{1}{2}, \dots, 45\}$, $N_V \le 12$, $N_P \le 2$ (145 509 contents, 7241 distinct pairs (X, Y); scripts `t14`, `t15`, `t21`). Results, for the optimised cutoff and within the scanned range:

- **Three admissible fixed points** occur for only 17 distinct (X, Y), the smallest content being $N_S = 1$, $N_D = 3/2$ ($X = 4$, $Y = -5$; e.g. one real scalar and three Weyl fermions): then $(g, \lambda) = (4.77, -0.713)$ (node, $\theta = 1.20, 2.49$), $(2.66, -0.100)$ (saddle, $\theta = 1.42, -1.27$), and $(1.39, 0.088)$ (focus, $\theta = 0.23 \pm 1.69i$), indices $(+1, -1, +1)$ as in Corollary 4.2. The full list of the 17 pairs, with their fixed points, is in `code/t22_tables.out`.

- **A UV-repulsive focus** ($\Re\theta < 0$ for a complex pair) occurs for 64 distinct (X, Y), e.g. $N_S = 3$, $N_D = 2$ ($X = 7$, $Y = -5$): $(g_*, \lambda_*) = (1.336, 0.116)$, $\theta = -0.013 \pm 2.062\,i$, just on the repulsive side of the Hopf curve ($Y_H(7) = -4.979$).

- The **periodic orbit** exists around the UV-attractive focus for the contents with smallest $\Re\theta > 0$: $(X, Y) = (63, -6)$ ($N_S = 40$, $N_D = 11.5$; $\Re\theta = 0.061$, orbit amplitude 0.18, period 0.72) and $(49, -5)$ ($N_S = 31$, $N_D = 9$; $\Re\theta = 0.121$, amplitude 0.39, period 0.88). The next ones, $\Re\theta = 0.14$–0.23 (e.g. $N_S = 14$, $N_D = 4.5$), have none. These contents need thirty or more scalar fields: they are not natural, and the result should not be read as a prediction for a realistic matter sector.

The Standard Model content ($X = 1$, $Y = -62$) and the QDG families have a single fixed point (Proposition 3.4).

9 Limits of validity and open problems

1. All statements are for the truncated Einstein–Hilbert flow; couplings $g_* \simeq 1$–2 at the BT point are not in the regime in which the truncation is controlled. The existence of the structures in an extended truncation (e.g. with R^2, in which the fixed point already has three exponents [3]) is not examined: there the stability matrix is 3×3 and the BT/Hopf analysis changes.

2. The cuspidal cubic and the index formula are exact for the flow (1)–(2); Theorem 3.3 uses the linearity of the fixed-point locus in (X, Y), which I took from the code of the book and checked numerically for one exponential regulator, not proved for general cutoffs.

3. The Bogdanov–Takens non-degeneracy ($a, b \neq 0$) and the sign of ℓ_1 are computed by finite differences; the periodic orbit and the homoclinic loop are numerical. A rigorous proof, e.g. by computing the BT normal form symbolically, is open.

4. The type-B matter counting, the gauge and the linear split are fixed. Whether the cusp and BT point persist for other gauges is unknown.

5. The Weyl-gauged QDG sector is not included.

6. The sliver of matter space in which the orbit exists is thin ($\sim 10^{-2}$ in Y near BT_1); any change of scheme shifts it, and it contains no integer content near BT_1.

10 Conclusions

For the derived Einstein–Hilbert flow with minimal matter, the fixed points form a ruled surface whose fold curve in the (X, Y) plane is a cuspidal cubic with a cusp at an exactly known rational point; the sign of the determinant of the stability matrix is the sign of the derivative of the fixed-point cubic; and the trace has a closed form from which a Bogdanov–Takens point at $(X, Y) \simeq (4.02, -5.35)$ and an algebraic Hopf curve follow. Numerically, the Hopf curve is subcritical and bounds, together with a homoclinic curve, a region in which the UV attractive focus is surrounded by an unstable periodic orbit of the flow. The cusp and the Bogdanov–Takens point persist for six regulators. None of this is reached by the matter contents assigned to QDG.

Acknowledgements. The author thanks the scientific community for discussions and feedback. This work was conducted without institutional or financial support. All calculations were performed in Python with NumPy and SciPy (exact rational arithmetic with the standard `fractions` module); no computer algebra system was available.

Author contributions. L. E. Pavesi: Conceptualization, Formal analysis, Investigation, Methodology, Writing – original draft preparation, Writing – review and editing.

A Scripts

All numbers are reproduced by the scripts in `code/` (NumPy, SciPy and Matplotlib only; outputs saved as `*.out`).

- `flow.py`: the flow, analytic Jacobian, fixed points; `t1_check.py`: Jacobian against finite differences, fixed points of the book.
- `t2_fold.py`, `t12_implicit.py`: fold curve, cusp, exact discriminant (Proposition 3.1); `t13_lines.py`, `t22_tables.py`: QDG families (Proposition 3.4).
- `t4_det.py`: Proposition 4.1; `ratfun.py`, `t3_bt.py`, `t19_hopf_closed.py`: Propositions 5.1, 5.2 and Eq. (11); `verify_all.py`: all exact statements.
- `t5_bt_normal.py`: BT coefficients; `lyap.py`, `t16_l1_global.py`: ℓ_1; `t6_hopf.py`, `make_curves.py`: Hopf curve.
- `cyc.py`, `t9_hom.py`, `t10_homcurve.py`, `t17_cycle_far.py`, `t18_homoclinic.py`: periodic orbit and homoclinic loop; `make_figs.py`, `make_fig3.py`: figures.
- `t20_regulators.py`, `t23_reg_trace_map.py`: other regulators; `t14_lattice.py`, `t15_lattice2.py`, `t21_lattice_cycles.py`: integer contents.

The core of the exact check of Propositions 3.1 and 4.1 is:

```
from fractions import Fraction as Fr
Xs = lambda s: 14-59*s**2+48*s**3
Ys = lambda s: 18-Fr(236,3)*s+Fr(262,3)*s**2-32*s**3
def F(u,X,Y):  c=14-X; return 2*c*u**3-(2*c+54-3*Y)*u**2+118*u-48
def Fp(u,X,Y): c=14-X; return 6*c*u**2-2*(2*c+54-3*Y)*u+118
assert all(F(1/s,Xs(s),Ys(s))==0 and Fp(1/s,Xs(s),Ys(s))==0 for s in [Fr(k,7) for k
    in range(1,30)])
```

References

[1] M. Reuter, *Nonperturbative Evolution Equation for Quantum Gravity*, Physical Review D **57** (1998) 971–985.

[2] D. F. Litim, *Optimised renormalisation group flows*, Physical Review D **64** (2001) 105007, arXiv:hep-th/0103195.

[3] O. Lauscher, M. Reuter, *Flow equation of quantum Einstein gravity in a higher-derivative truncation*, Physical Review D **66** (2002) 025026, arXiv:hep-th/0205062.

[4] P. Donà, A. Eichhorn, R. Percacci, *Matter matters in asymptotically safe quantum gravity*, Physical Review D **89** (2014) 084035, arXiv:1311.2898.

[5] H. Whitney, *On singularities of mappings of Euclidean spaces. I. Mappings of the plane into the plane*, Annals of Mathematics **62** (1955) 374–410.

[6] F. Takens, *Singularities of vector fields*, Publications Mathématiques de l'IHÉS **43** (1974) 47–100.

[7] R. I. Bogdanov, *Versal deformations of a singular point of a vector field on the plane in the case of zero eigenvalues*, Functional Analysis and Its Applications **9** (1975) 144–145 (Funktsional. Anal. i Prilozhen. **9**, no. 2, 63).

[8] Yu. A. Kuznetsov, *Elements of Applied Bifurcation Theory*, 4th ed., Applied Mathematical Sciences **112**, Springer (2023), doi:10.1007/978-3-031-22007-4.

[9] L. E. Pavesi, Quantum Distortion Gravity, second edition, Part IV (chapters on the Einstein–Hilbert flow, minimally coupled matter, the fixed point, matter, regulator and truncation dependence, and the model flow) and the chapter on regulator-robust existence (2026).